Available online at www.sciencedirect.com
ScienceDirect
Journal of Power Sources 178 (2008) 353–362
JOURNAL OF POWER SOURCES
www.elsevier.com/locate/jpowsour

Short communication

Flow distribution in U-type layers or stacks of planar fuel cells

Wen Lai Huang *, Qingshan Zhu

State Key Laboratory of Multi-Phase Complex Systems, Institute of Process Engineering, Chinese Academy of Sciences, Zhong Guan Cun, Haidian District, P.O. Box 353, Beijing 100080, People's Republic of China

Received 1 November 2007; received in revised form 2 December 2007; accepted 3 December 2007
Available online 8 December 2007

Abstract

The flow distribution features in U-type layers or stacks with certain practical configurations have been investigated analytically. The formulations suggest general designing strategies to improve the flow uniformity, and narrowing some positions of the channels proves effective. The flow uniformity among the layers in a U-type stack is relatively easy to achieve in comparison with that among the channels in a U-type layer, due to the large stack headers and low-pressure loss in them. CFD simulations confirm the formulations, and the discrepancies between the analytical and CFD results have been attributed to the ignored factors during the analytical formulations.

Keywords: Flow distribution; U-type parallel channel; Laminar flow; Planar fuel cells

1. Introduction

The flow-distribution uniformity is a basic target in fuel-cell design and manipulations, and various configurations have emerged to improve the performance. The most popular method for design optimization is usually based on numerical techniques, adopting commercial CFD (computational fluid dynamics) codes [1–4], for the cases are normally too complicated to treat analytically. However, analytical solutions are extremely desirable if available because of their straightforward and fast solving and possibly revealing definite relations among quantities. Fortunately, certain configurations have been reported with analytical solutions, based on some simplifications, including the well-known Z-type and U-type parallel channels [5,6]. Based on analytical formulations, Sung [7] has further proposed optimized header shapes to improve the flow distributions.

Thanks to the difficulties in treating complex pressure losses, the analytical formulations reported so far are mainly emphasized on relatively simple configurations, and at the layer level. Meanwhile, more complex configurations are popular in practice, and analysis on a fuel-cell stack is commonly as necessary as on a layer, for flow distribution among the layers in a large stack can play a controlling role on the overall performance. With certain simplifications and assumptions, the present work attempts to formulate analytically in some more complex cases. Since the U-type configuration is more efficient than the Z-type one in improving the flow uniformity [5], and more widely adopted in fuel-cell stacks, U-type layers and stacks are the focus here. Comparisons with CFD simulations will also be discussed.

2. Formulation

Certain assumptions are employed in the following formulations. The density ρ and dynamic viscosity μ of the fluid are assumed to be constant, i.e., the flow is assumed to be incompressible and the temperature is assumed to be uniform. The gas consumption, leakage or transformation is not taken into account, and the mass conservation is assumed in the whole flow field. The flow is assumed to be laminar, and the inertial term is neglected during considering the momentum balance. The local losses are neglected in all cases, including the dividing, combining, expanding and contracting ones. Especially in the stack cases, the pressure loss in the layer headers has also been neglected to simplify the formulation. And for convenience, the feed header in present work is assumed to have the same size as the exhaust header.

* Corresponding author. Tel.: +86 10 62650558; fax: +86 10 62536108.
E-mail address: wlhuang@home.ipe.ac.cn (W.L. Huang).

0378-7753/$ – see front matter © 2007 Elsevier B.V. All rights reserved.
doi:10.1016/j.jpowsour.2007.12.003

Nomenclature

a	aspect ratio
A	cross-sectional area
D	hydraulic diameter
f	friction factor
F	flow parameter index
$g(F)$	function of F in Eq. (40), etc.
G_1	constant in Eq. (14a), etc.
G_2	constant in Eq. (14b), etc.
H	height or depth
K_0	intermediate quantity in Eq. (6), etc.
K_1	dimensionless quantity in Eq. (9a), etc.
K_2	dimensionless quantity in Eq. (9b), etc.
l	overall loss coefficient
L	length
N	number
p	pressure
P	perimeter
r	constant in Eq. (15), etc.
Re	Reynolds number
s	constant in Eq. (15), etc.
u	velocity
W	width
x	Cartesian coordinate

Greek letters

λ_{fric}	frictional loss coefficient
μ	dynamic viscosity
ρ	density
ζ_t	turning loss factor

Subscripts

avg	average
c	channel
c1	channel part 1
c2	channel part 2
e	exhaust
f	feed
h	header
in	inlet
layer	layer
max	maximum
min	minimum
r	rib
stack	stack

Cap

ˆ	dimensionless

2.1. U-type layer with uniform channels

The formulation in this section involves the U-type configuration containing channels with uniform shape (Fig. 1, called "case1-0"), basically according to the work in Ref. [5].

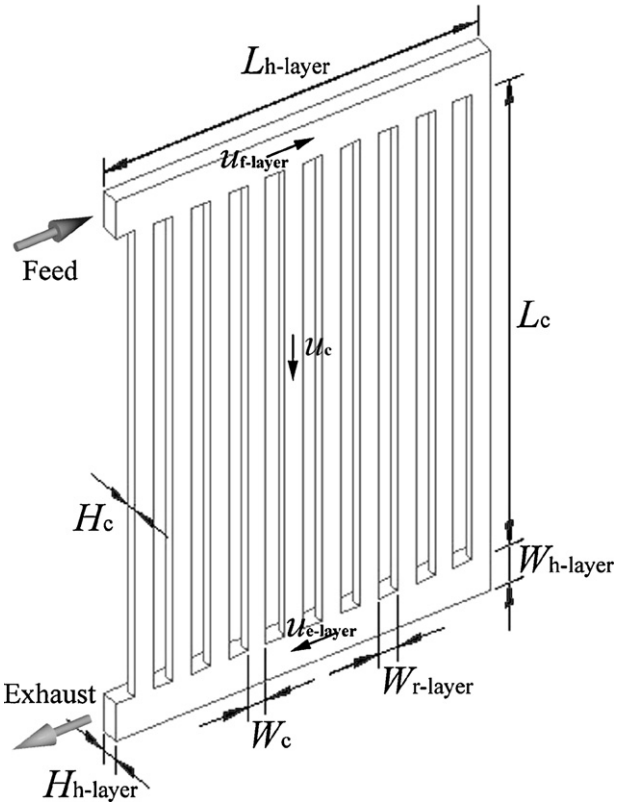

Fig. 1. The U-type layer with uniform channels (case1-0).

Mass balance requires

$$A_{h\text{-layer}}\frac{du_{f\text{-layer}}}{dx_{f\text{-layer}}} = -\frac{N_c}{L_{h\text{-layer}}}u_c A_c \tag{1a}$$

for the feed header and

$$A_{h\text{-layer}}\frac{du_{e\text{-layer}}}{dx_{e\text{-layer}}} = -\frac{N_c}{L_{h\text{-layer}}}u_c A_c \tag{1b}$$

for the exhaust header, where A, u, x, N and L stand for the cross-sectional area, the velocity, the distance from the inlet, the number, and the length, respectively, and the subscripts "h", "f", "e", "layer" and "c" means "header", "feed", "exhaust", "layer" and "channel", respectively. With the ignorance of the inertial term [5], the momentum balance requires

$$\frac{d}{dx_{f\text{-layer}}}(\rho u_{f\text{-layer}}^2) = -\frac{dp_{f\text{-layer}}}{dx_{f\text{-layer}}} - \frac{P_{h\text{-layer}} f_{h\text{-layer}} \rho u_{f\text{-layer}}^2}{2A_{h\text{-layer}}} \tag{1c}$$

for the feed header and

$$\frac{d}{dx_{e\text{-layer}}}(\rho u_{e\text{-layer}}^2) = -\frac{dp_{e\text{-layer}}}{dx_{e\text{-layer}}} + \frac{P_{h\text{-layer}} f_{h\text{-layer}} \rho u_{e\text{-layer}}^2}{2A_{h\text{-layer}}} \tag{1d}$$

for the exhaust header, where p, P and f represent the pressure, the perimeter and the friction factor, respectively. Considering

$$p_{f\text{-layer}} - p_{e\text{-layer}} = \Delta p_{f\text{-e-layer}} = l_c \frac{1}{2}\rho u_c^2 \tag{2}$$

while

$$l_c = \zeta_{t\text{-}f} + \zeta_{t\text{-}e} + \lambda_{fric\text{-}c} \approx \lambda_{fric\text{-}c} \tag{3}$$

$$\lambda_{fric\text{-}c} = \frac{4 f_c L_c}{D_c} \tag{4}$$

where l_c is the overall loss coefficient in the channel, $\zeta_{t\text{-}f}$ and $\zeta_{t\text{-}e}$ are the turning loss factors for flow dividing and combining, $\lambda_{fric\text{-}c}$ is the frictional loss coefficient in the channel, and D is the hydraulic diameter. Neglecting $\zeta_{t\text{-}f}$ and $\zeta_{t\text{-}e}$ in Eq. (3) is based on the low Reynolds number (laminar flow) and the high length to diameter ratio of the channel ($L_c/D_c > 100$) [5] investigated here. Using the empirical correlation

$$Ref = 13.84 + 10.38 \exp\left(\frac{-3.4}{a}\right) \tag{5}$$

where a is the channel aspect ratio. According to Eqs. (2)–(4) and the definition of Reynolds number, the relation between u_c and $\Delta p_{f\text{-}e\text{-}layer}$ can be derived as

$$\Delta p_{f\text{-}e\text{-}layer} = u_c \left(\frac{2\mu L_c (Ref)_c}{{D_c}^2}\right) = \frac{u_c}{K_0} \tag{6}$$

where μ is the dynamic viscosity of the fluid. With the following nondimensionalizaion:

$$\hat{x} = \frac{x}{L_{h\text{-}layer}} \tag{7a}$$

$$\hat{u} = \frac{u}{u_{in\text{-}layer}} \tag{7b}$$

$$\hat{p} = \frac{p}{\rho u_{in\text{-}layer}^2} \tag{7c}$$

Eqs. (1a)–(1d) evolve as a set of ordinary differential equations:

$$\frac{d\hat{u}_{f\text{-}layer}}{d\hat{x}} = -K_1 \Delta \hat{p}_{f\text{-}e\text{-}layer} \tag{8a}$$

$$\frac{d\hat{u}_{e\text{-}layer}}{d\hat{x}} = -K_1 \Delta \hat{p}_{f\text{-}e\text{-}layer} \tag{8b}$$

$$2\hat{u}_{f\text{-}layer}\frac{d\hat{u}_{f\text{-}layer}}{d\hat{x}} + \frac{d\hat{p}_{f\text{-}layer}}{d\hat{x}} + K_2 \hat{u}_{f\text{-}layer} = 0 \tag{8c}$$

$$2\hat{u}_{e\text{-}layer}\frac{d\hat{u}_{e\text{-}layer}}{d\hat{x}} + \frac{d\hat{p}_{e\text{-}layer}}{d\hat{x}} - K_2 \hat{u}_{e\text{-}layer} = 0 \tag{8d}$$

where

$$K_1 = \frac{N_c \rho u_{in\text{-}layer} A_c}{A_{h\text{-}layer}} K_0 = \frac{N_c \rho u_{in\text{-}layer}}{2\mu} \frac{A_c D_c^2}{(Re\ f)_c L_c A_{h\text{-}layer}} \tag{9a}$$

$$K_2 = \frac{P_{h\text{-}layer}\mu (Ref)_{h\text{-}layer} L_{h\text{-}layer}}{2A_{h\text{-}layer} D_{h\text{-}layer} \rho u_{in\text{-}layer}} = \frac{2\mu}{\rho u_{in\text{-}layer}} \frac{(Ref)_{h\text{-}layer} L_{h\text{-}layer}}{D_{h\text{-}layer}^2} \tag{9b}$$

According to the continuity equation

$$\hat{u}_{f\text{-}layer} = \hat{u}_{e\text{-}layer} \tag{10}$$

A second-order differential equation is derived as following

$$\frac{d^2 \hat{u}_{f\text{-}layer}}{d\hat{x}^2} - 2K_1 K_2 \hat{u}_{f\text{-}layer} = 0 \tag{11}$$

Using the boundary conditions

$$\hat{x} = 0, \quad \hat{u}_{f\text{-}layer} = 1 \tag{12a}$$

$$\hat{x} = 1, \quad \hat{u}_{f\text{-}layer} = 0 \tag{12b}$$

the resultant solution is

$$\hat{u}_{f\text{-}layer} = G_1 e^{r\hat{x}} + G_2 e^{s\hat{x}} \tag{13}$$

where

$$G_1 = \frac{e^s}{e^s - e^r} \tag{14a}$$

$$G_2 = \frac{e^r}{e^r - e^s} \tag{14b}$$

and

$$r = -s = \sqrt{2K_1 K_2} \tag{15}$$

Meanwhile, the following results can be obtained

$$\Delta \hat{p}_{f\text{-}e\text{-}layer} = -\frac{G_1 r e^{r\hat{x}} + G_2 s e^{s\hat{x}}}{K_1} \tag{16}$$

$$\hat{m}_c = -\frac{G_1 r e^{r\hat{x}} + G_2 s e^{s\hat{x}}}{N_c} \tag{17}$$

where $\hat{m}$ is the dimensionless relative flow rate. The following parameter can be utilized to evaluate the uniformity of flow distribution

$$F_c = \frac{\hat{m}_{c\text{-}max} - \hat{m}_{c\text{-}min}}{\hat{m}_{c\text{-}max}} \tag{18}$$

2.2. U-type layer with complex channels

During practical manufacturing, complex channels might be selected owing to the technical limitations or cost considerations. If certain shape change can improve the flow distribution, it is certainly further desirable.

The first case considered here is that each channel consists of three parts (Fig. 2, called "case1-1"). The two parts connected respectively to the feed and exhaust headers are of the same size and called "c1" while the middle channel is called "c2". Hence, this kind of channel is named as "c1 + c2 + c1" type in the present work. For convenience, the "c1" here and hereafter has the same width as "c2".

When the local losses described in Eq. (3) and those across the two channel parts (expanding and contracting losses) are neglected, the following relationship can be derived:

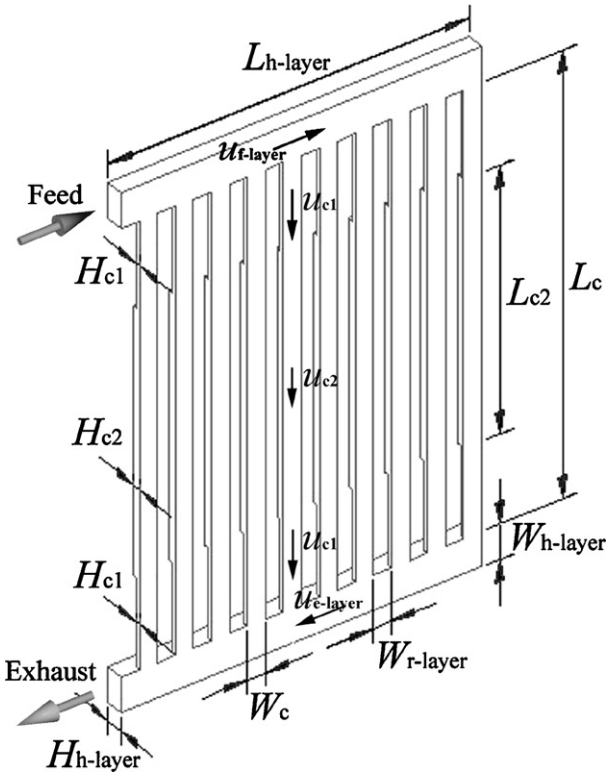

Fig. 2. The U-type layer with "c1 + c2 + c1" channels (case1-1).

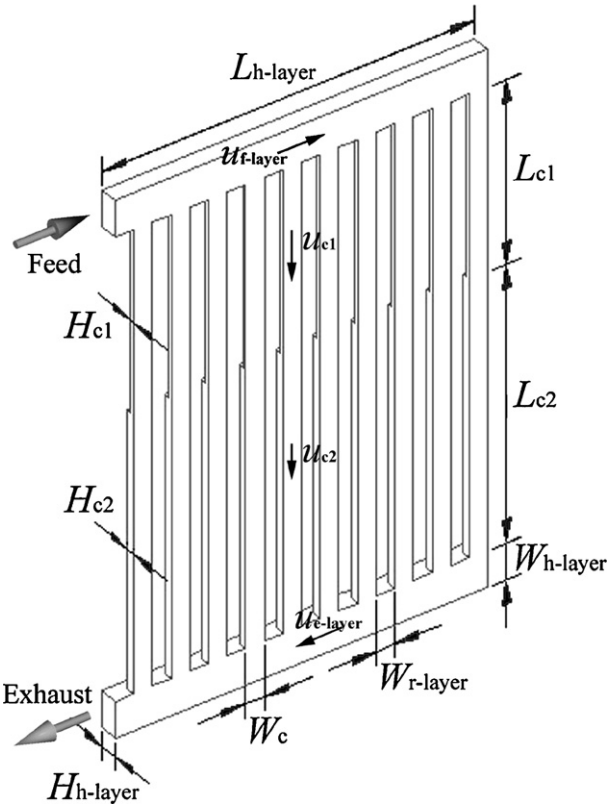

Fig. 3. The U-type layer with "c1 + c2" channels (case1-2).

$$\Delta p_{\text{f-e-layer}} = 2\mu\left(\frac{L_{c1}(Ref)_{c1}}{D_{c1}^2} + \frac{L_{c2}(Ref)_{c2}}{D_{c2}^2}\frac{A_{c1}}{A_{c2}}\right)$$

$$u_{c1} = \frac{u_{c1}}{K_0} \tag{19}$$

where $L_{c1} = L_c - L_{c2}$, is the total length of "c1" in a channel. In this case, mass balance gives the following relations:

$$A_{\text{h-layer}}\frac{du_{\text{f-layer}}}{dx_{\text{f-layer}}} = -\frac{N_c}{L_{\text{h-layer}}}u_{c1}A_{c1} \tag{20a}$$

$$A_{\text{h-layer}}\frac{du_{\text{e-layer}}}{dx_{\text{e-layer}}} = -\frac{N_c}{L_{\text{h-layer}}}u_{c1}A_{c1} \tag{20b}$$

while the momentum balance provides the same equations as Eqs. (1c) and (1d). Eqs. (8a)–(8d) can also be derived with

$$K_1 = \frac{N_c\rho u_{\text{in-layer}}A_{c1}}{A_{\text{h-layer}}}K_0 = \frac{N_c\rho u_{\text{in-layer}}}{2\mu}\left(\frac{1}{L_{c1}(Re\ f)_{c1}/A_{c1}D_{c1}^2 + L_{c2}(Re\ f)_{c2}/A_{c2}D_{c2}^2}\right)\frac{1}{A_{\text{h-layer}}} \tag{21}$$

and the same expression of K_2 in Eq. (9b). After solving, the same results as expressed in Eqs. (16) and (17) can be obtained.

Compared with case1-0, it is observed that partitioning the channel into different parts has brought extra term into the pressure loss along the channels, helping to tailor the flow distribution.

The next case for investigation is that the channel consists of only two parts ("c1" and "c2") connecting the inlet and exhaust header, respectively (Fig. 3, called "case1-2"), and such channel is called "c1 + c2" type hereinafter.

In this case, the same relationship as Eq. (19) holds if the local losses are neglected. The mass balance gives Eq. (20a) for the feed header, and the following

$$A_{\text{h-layer}}\frac{du_{\text{e-layer}}}{dx_{\text{e-layer}}} = -\frac{N_c}{L_{\text{h-layer}}}u_{c2}A_{c2} = -\frac{N_c}{L_{\text{h-layer}}}u_{c1}A_{c1} \tag{22}$$

for the exhaust header due to $u_{c1}\,A_{c1} = u_{c2}\,A_{c2}$.The further formulation is the same as the above case1-1 with K_1 expressed in Eq. (21), K_2 in Eq. (9b), and the results in Eqs. (16) and (17).

More complex channel shape can also be analyzed using the same formulating procedure as above. For any types of channels containing different parts, the frictional loss corresponding to each part can be considered, respectively, and the only correction is within the K_1 expression when the turning, dividing, combining, expanding and contracting losses are neglected.

2.3. U-type stack with parallel layers

U-type stacks are frequently encountered, for the feeding and exhausting are usually conducted on the same manifold platform to easy the gas manipulation. The flow distribution among layers is never less important than that among channels. Fortunately, U-type stacks are very analogous to U-type layers, and the formulation becomes timesaving on the basis of the preceding sections.

First, uniform channels are investigated. A fuel-cell stack is considered with layers forming a U-type configuration, while

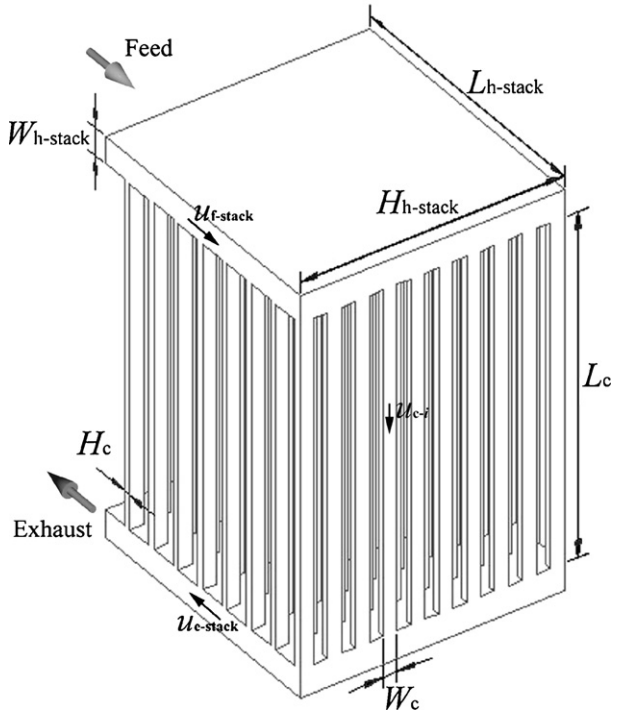

Fig. 4. The U-type stack with uniform channels (case2-0).

each layer contains the same uniform channels (Fig. 4, called "case2-0").

In order to investigate the flow distribution among the layers, the mass balance and momentum balance in the stack are considered as follows

$$A_{\text{h-stack}}\frac{\mathrm{d}u_{\text{f-stack}}}{\mathrm{d}x_{\text{f-stack}}} = -\frac{N_{\text{layer}}}{L_{\text{h-stack}}}u_{\text{layer}}A_{\text{layer}} = -\frac{N_{\text{layer}}}{L_{\text{h-stack}}}u_{\text{c-avg}}N_{\text{c}}A_{\text{c}} \tag{23a}$$

$$A_{\text{h-stack}}\frac{\mathrm{d}u_{\text{e-stack}}}{\mathrm{d}x_{\text{e-stack}}} = -\frac{N_{\text{layer}}}{L_{\text{h-stack}}}u_{\text{layer}}A_{\text{layer}} = -\frac{N_{\text{layer}}}{L_{\text{h-stack}}}u_{\text{c-avg}}N_{\text{c}}A_{\text{c}} \tag{23b}$$

$$\frac{\mathrm{d}}{\mathrm{d}x_{\text{f-stack}}}(\rho u_{\text{f-stack}}^2) = -\frac{\mathrm{d}p_{\text{f-stack}}}{\mathrm{d}x_{\text{f-stack}}} - \frac{P_{\text{h-stack}}f_{\text{h-stack}}\rho u_{\text{f-stack}}^2}{2A_{\text{h-stack}}} \tag{23c}$$

$$\frac{\mathrm{d}}{\mathrm{d}x_{\text{e-stack}}}(\rho u_{\text{e-stack}}^2) = -\frac{\mathrm{d}p_{\text{e-stack}}}{\mathrm{d}x_{\text{e-stack}}} + \frac{P_{\text{h-stack}}f_{\text{h-stack}}\rho u_{\text{e-stack}}^2}{2A_{\text{h-stack}}} \tag{23d}$$

where the subscript "stack" means the stack, N_{layer} is the number of layers, N_{c} is the number of channels in one layer, u_{layer} is considered as $u_{\text{c-avg}}$ (the average u_{c}, $u_{\text{c-avg}} = (1/N_{\text{c}})\sum_{i=1}^{N_{\text{c}}}u_{\text{c-}i}$), and $A_{\text{layer}} = N_{\text{c}}\ A_{\text{c}}$. Meanwhile, the relationship between $u_{\text{c-avg}}$ and $\Delta p_{\text{f-e-stack}}$ can be derived as

$$\Delta p_{\text{f-e-stack}} = l_{\text{layer}}\frac{1}{2}\rho u_{\text{layer}}^2 \approx N_{\text{c}}u_{\text{c-avg}}\left(\frac{2\mu L_{\text{c}}(Ref)_{\text{c}}}{D_{\text{c}}^2}\right) = \frac{N_{\text{c}}u_{\text{c-avg}}}{K_0} \tag{24}$$

based on the assumption that

$$l_{\text{layer}} \approx \lambda_{\text{fric-layer}} = N_{\text{c}}\frac{4f_{\text{c}}L_{\text{c}}}{D_{\text{c}}} \tag{25}$$

and $u_{\text{layer}} = u_{\text{c-avg}}$. After nondimensionalization as follows,

$$\hat{x} = \frac{x}{L_{\text{h-stack}}} \tag{26a}$$

$$\hat{u} = \frac{u}{u_{\text{in-stack}}} \tag{26b}$$

$$\hat{p} = \frac{p}{\rho u_{\text{in-stack}}^2} \tag{26c}$$

the following equations can be achieved.

$$\frac{\mathrm{d}\hat{u}_{\text{f-stack}}}{\mathrm{d}\hat{x}} = -K_1\Delta\hat{p}_{\text{f-e-stack}} \tag{27a}$$

$$\frac{\mathrm{d}\hat{u}_{\text{e-stack}}}{\mathrm{d}\hat{x}} = -K_1\Delta\hat{p}_{\text{f-e-stack}} \tag{27b}$$

$$2\hat{u}_{\text{f-stack}}\frac{\mathrm{d}\hat{u}_{\text{f-stack}}}{\mathrm{d}\hat{x}} + \frac{\mathrm{d}\hat{p}_{\text{f-stack}}}{\mathrm{d}\hat{x}} + K_2\hat{u}_{\text{f-stack}} = 0 \tag{27c}$$

$$2\hat{u}_{\text{e-stack}}\frac{\mathrm{d}\hat{u}_{\text{e-stack}}}{\mathrm{d}\hat{x}} + \frac{\mathrm{d}\hat{p}_{\text{e-stack}}}{\mathrm{d}\hat{x}} - K_2\hat{u}_{\text{e-stack}} = 0 \tag{27d}$$

where

$$K_1 = \frac{N_{\text{layer}}\rho u_{\text{in-stack}}A_{\text{c}}}{A_{\text{h-stack}}}\quad K_0 = \frac{N_{\text{layer}}\rho u_{\text{in-stack}}}{2\mu}\quad \frac{A_{\text{c}}D_{\text{c}}^2}{(Re\ f)_{\text{c}}L_{\text{c}}A_{\text{h-stack}}} \tag{28a}$$

$$K_2 = \frac{P_{\text{h-stack}}\mu(Ref)_{\text{h-stack}}L_{\text{h-stack}}}{2A_{\text{h-stack}}D_{\text{h-stack}}\rho u_{\text{in-stack}}} = \frac{2\mu}{\rho u_{\text{in-stack}}}\quad \frac{(Ref)_{\text{h-stack}}L_{\text{h-stack}}}{D_{\text{h-stack}}^2} \tag{28b}$$

Using the continuity condition

$$\hat{u}_{\text{f-stack}} = \hat{u}_{\text{e-stack}} \tag{29}$$

and the boundary conditions

$$\hat{x} = 0,\quad \hat{u}_{\text{f-stack}} = 1 \tag{30a}$$

$$\hat{x} = 1,\quad \hat{u}_{\text{f-stack}} = 0 \tag{30b}$$

the solution is

$$\hat{u}_{\text{f-stack}} = G_1e^{r\hat{x}} + G_2e^{s\hat{x}} \tag{31}$$

and

$$\Delta\hat{p}_{\text{f-e-stack}} = -\frac{G_1re^{r\hat{x}} + G_2se^{s\hat{x}}}{K_1} \tag{32}$$

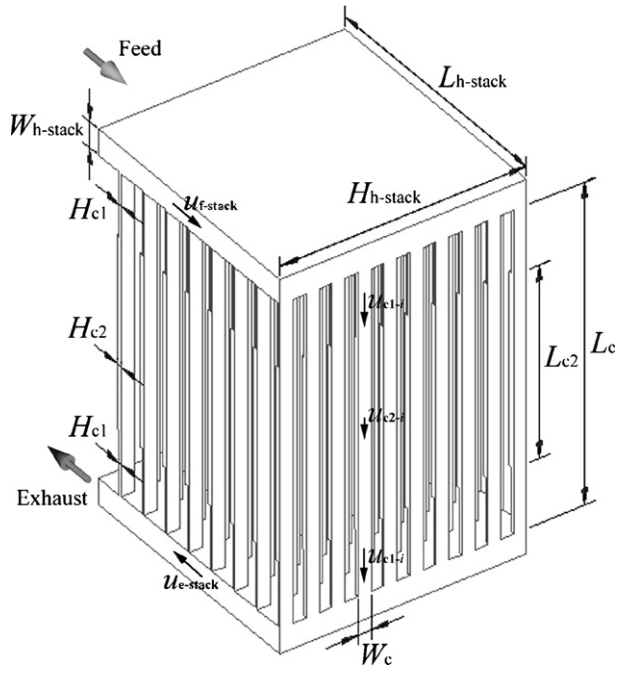

Fig. 5. The U-type stack with "c1 + c2 + c1" channels (case2-1).

$$\hat{m}_{\text{layer}} = -\frac{G_1 r e^{r\hat{x}} + G_2 s e^{s\hat{x}}}{N_{\text{layer}}} \tag{33}$$

with the same definitions as in Eqs. (14) and (15), and the flow distribution among the layers can be evaluated using

$$F_{\text{layer}} = \frac{\hat{m}_{\text{layer-max}} - \hat{m}_{\text{layer-min}}}{\hat{m}_{\text{layer-max}}} \tag{34}$$

Given a glance at the expressions of K_1 and K_2 in Eqs. (28a) and (28b), it is easy to find that besides channels, the flow distribution among layers is dominated by the stack headers here instead of layer headers in the layer cases. This makes it easier to achieve a better flow distribution among layers than among channels due to the usually larger size of stack headers than layer headers.

Next, we begin to analyze the stacks containing complex channels. The first case is that each channel consists of three parts, i.e., "c1 + c2 + c1" (Fig. 5, called "case2-1").

Similar to the above analyses, the following equations can be deduced based on mass balance:

$$A_{\text{h-stack}}\frac{\mathrm{d}u_{\text{f-stack}}}{\mathrm{d}x_{\text{f-stack}}} = -\frac{N_{\text{layer}}}{L_{\text{h-stack}}}u_{\text{layer}}A_{\text{layer}} = -\frac{N_{\text{layer}}}{L_{\text{h-stack}}}u_{\text{c1-avg}}N_{\text{c}}A_{\text{c1}} \tag{35a}$$

$$A_{\text{h-stack}}\frac{\mathrm{d}u_{\text{e-stack}}}{\mathrm{d}x_{\text{e-stack}}} = -\frac{N_{\text{layer}}}{L_{\text{h-stack}}}u_{\text{layer}}A_{\text{layer}} = -\frac{N_{\text{layer}}}{L_{\text{h-stack}}}u_{\text{c1-avg}}N_{\text{c}}A_{\text{c1}} \tag{35b}$$

where u_{layer} is considered as $u_{\text{c1-avg}}$ (the average u_{c1}, $u_{\text{c1-avg}} = (1/N_{\text{c}})\sum_{i=1}^{N_{\text{c}}} u_{\text{c1}-i}$), and $A_{\text{layer}} = N_{\text{c}}A_{\text{c1}}$. The momentum balance gives the same equations as Eqs. (23c) and (23d). Once only the frictional loss is considered, the relationship between $u_{\text{c1-avg}}$ and $\Delta p_{\text{f-e-stack}}$ can be derived as

$$\Delta p_{\text{f-e-stack}} = 2\mu\left(\frac{L_{\text{c1}}(Ref)_{\text{c1}}}{{D_{\text{c1}}}^2} + \frac{L_{\text{c2}}(Ref)_{\text{c2}}}{{D_{\text{c2}}}^2}\frac{A_{\text{c1}}}{A_{\text{c2}}}\right)$$

$$N_{\text{c}}u_{\text{c1-avg}} = \frac{N_{\text{c}}u_{\text{c1-avg}}}{K_0} \tag{36}$$

Subsequently, the deduced differential equations are same as Eqs. (27a)–(27d) with nondimensionalization as expressed in Eqs. (26a)–(26c) and K_2 in Eq. (28b), while K_1 as follows.

$$K_1 = \frac{N_{\text{layer}}\rho u_{\text{in-stack}}A_{\text{c1}}}{A_{\text{h-stack}}}K_0 = \frac{N_{\text{layer}}\rho u_{\text{in-stack}}}{2\mu}\left(\frac{1}{L_{\text{c1}}(Re\ f)_{\text{c1}}/A_{\text{c1}}D_{\text{c1}}^2 + L_{\text{c2}}(Re\ f)_{\text{c2}}/A_{\text{c2}}D_{\text{c2}}^2}\right)\frac{1}{A_{\text{h-stack}}} \tag{37}$$

Based on the continuity and boundary conditions shown in Eqs. (30), the solutions give the same expressions as in Eqs. (32) and (33).

Secondly, each channel is considered to be the "c1 + c2" type (Fig. 6, called "case2-2"), with "c2" connecting the exhaust header.

The mass balance for the exhaust header gives

$$A_{\text{h-stack}}\frac{\mathrm{d}u_{\text{e-stack}}}{\mathrm{d}x_{\text{e-stack}}} = -\frac{N_{\text{layer}}}{L_{\text{h-stack}}}u_{\text{c2-avg}}N_{\text{c}}A_{\text{c2}} = -\frac{N_{\text{layer}}}{L_{\text{h-stack}}}u_{\text{c1-avg}}N_{\text{c}}A_{\text{c1}} \tag{38}$$

according to $u_{\text{c1-avg}}\ A_{\text{c1}} = u_{\text{c2-avg}}A_{\text{c2}}$, where $u_{\text{c2}} = (1/N_{\text{c}})\sum_{i=1}^{N_{\text{c}}} u_{\text{c2}-i}$. Further formulation is the same as the above case2-1.

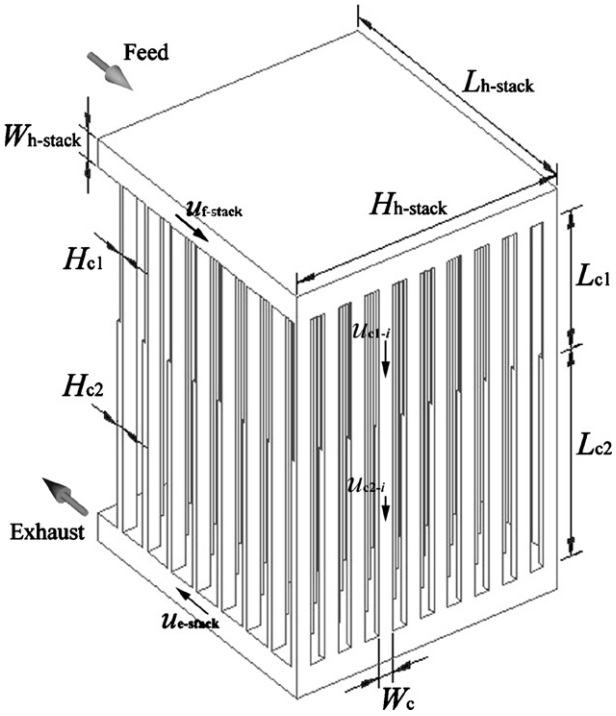

Fig. 6. The U-type stack with "c1 + c2" channels (case2-2).

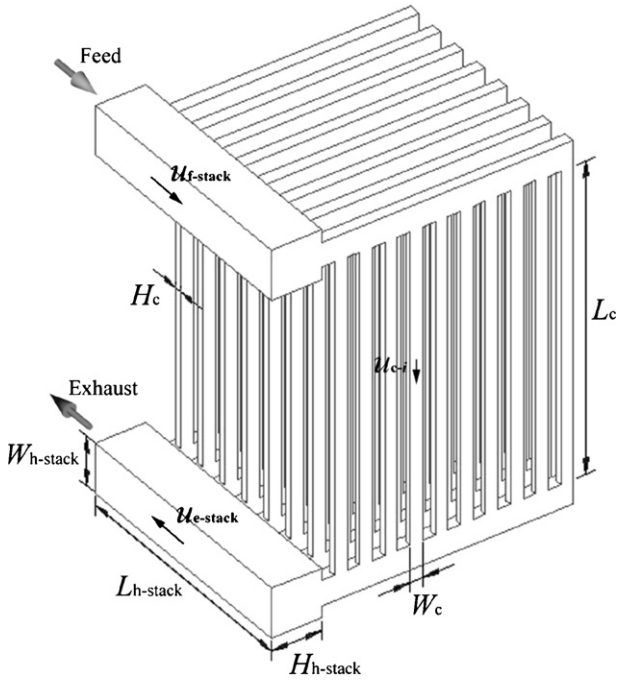

Fig. 7. The U-type stack with U-type layers with uniform channels (case3-0).

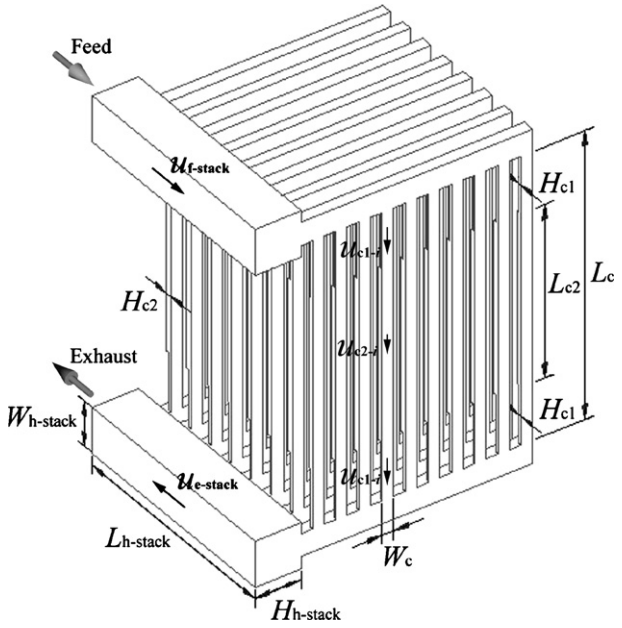

Fig. 8. The U-type stack with U-type layers with "c1 + c2 + c1" channels (case3-1).

2.4. U-type stack with U-type layers

Now, we explore a more complex configuration: a U-type stack built by U-type layers. Firstly, the channels are considered to be uniform (Fig. 7, called "case3-0"). The same equations as in Eqs. (23a)–(23d) can be obtained when assuming the u_{layer} as $u_{\text{c-avg}} = (1/N_c)\sum_{i=1}^{N_c} u_{\text{c-}i}$. And when neglecting the pressure loss in the layer headers, the same expression of K_1 as Eq. (28a) can also be deduced. With the same expression of K_2 as Eq. (28b), the results are the same as Eqs. (32) and (33).

When the channels are of the "c1 + c2 + c1" type (Fig. 8, called "case3-1"), the formulation is same as "case2-1". And if the channels belong to the "c1 + c2" type (Fig. 9, called "case3-2"), the formulation is same as in "case2-2".

3. Discussion and validation

3.1. Dependence of F on K_1 and K_2

As a simplification, $\hat{m}_{\max}$ and $\hat{m}_{\min}$ may be assigned to the values of $\hat{m}$ at $\hat{x} = 0$ and 1, respectively, during the calculation of F. Based on the above simplification and Eqs. (14), (15), (17) and (33),

$$F = 1 - \frac{G_1 r e^r + G_2 s e^s}{G_1 r + G_2 s} = 1 - \frac{2e^r}{1 + e^{2r}} \tag{39}$$

Hence,

$$e^r = \frac{1 + \sqrt{F(2-F)}}{1 - F} = g(F) \tag{40}$$

And according to Eq. (15), the following relation can be deduced.

$$\log K_2 + \log K_1 = 2\log(\ln g(F)) - \log 2 \tag{41}$$

For a given F, $\log K_2 \sim \log K_1$ appears as a line with slope of -1, as shown in Fig. 10. In other words, a line with slope of -1 in the $\log K_2 \sim \log K_1$ plot represents a same F value. More accurately, $\hat{m}_{\max}$ and $\hat{m}_{\max}$ can be calculated as the mean values in the first and last channels (or layers), respectively, for layer cases (or stack cases). However, for a definite configuration, the

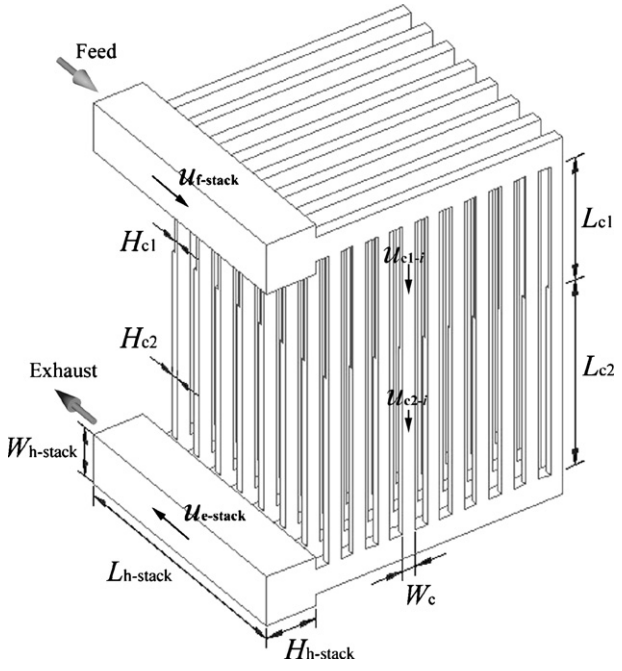

Fig. 9. The U-type stack with U-type layers with "c1 + c2" channels (case3-2).

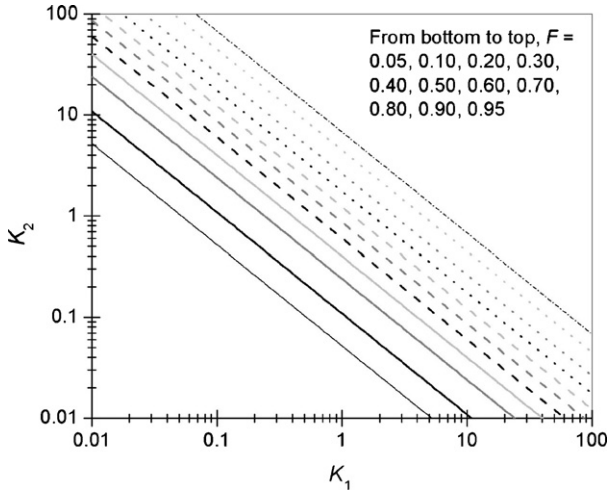

Fig. 10. Dependence of F on K_1 and K_2, based on simplified calculations.

relation between e^r and F is monotonous, and $\log K_2 \sim \log K_1$ will still appear as a line with slope of -1, and only certain (usually slight) difference in the intercept compared with the present simplified results.

3.2. Effects of the parameters on flow distribution

According to Eq. (41) and Fig. 10, it is obvious that in order to reduce F and obtain more uniform flow distribution, the product of K_1 and K_2 should be reduced. For the cases with uniform channels (case1-0, 2-0 and 3-0), a general expression for K_1K_2 can be given as follows.

$$K_1K_2 = N\frac{A_c {D_c}^2}{(Re\ f)_c L_c}\frac{(Re\ f)_h L_h}{A_h {D_h}^2} \tag{42}$$

It is readily found that to obtain smaller F and thus K_1 K_2, one needs smaller N, longer and finer channels with larger aspect ratio, and shorter and coarser headers with smaller aspect ratio. The subscript "h" here represents the layer header when considering the flow distribution among channels in a layer, or the stack header when considering the flow among layers in a stack. Since a stack header is often larger than a layer header, the flow distribution among the layers is usually more uniform than that among the channels. The variant u_{in} and the fluid features (ρ, μ) have not appeared in the above expression, and thus these parameters cannot affect the flow distribution as reported by other authors [5].

For the channels consisting of two different parts (both "c1 + c2 + c1" and "c1 + c2" types, i.e., case1-1, 1-2, 2-1, 2-2, 3-1 and 3-2), the product of K_1 and K_2 is expressed in Eq. (43), and the two parts now both contribute to the flow distribution. And according to the expression, each part needs to be fine, long and of large aspect ratio to achieve a uniform flow.

$$K_1K_2 = N\frac{1}{(Ref)_{c1}L_{c1}/A_{c1}D_{c1}^2 + (Ref)_{c2}L_{c2}/A_{c2}D_{c2}^2}\frac{(Ref)_h L_h}{A_h D_h^2} \tag{43}$$

3.3. Applications and validations

Some examples of the above-mentioned cases are given in Table 1, along with the corresponding analytical results. For convenience, the F values in Table 1 were calculated using the mass flow rates at the channel centers. The results are in accordance with the discussions in the above section, and it is obvious that changes in the channel size can tailor the flow uniformity effectively.

The validation of the analytical formulations depends on the correctness of the related assumptions. During the formulation, several assumptions have been made, analyses of which will aid to understand the corresponding validations.

An assumption is the neglecting of the inertial term during building the momentum balance equations. In the case of turbulent flow, Bassiouny and Martin [8,9] neglected the frictional

Table 1
The flow distribution in different cases (dimensions in mm)

Case1-0

$L_{h\text{-layer}}$	$W_{h\text{-layer}}$	$H_{h\text{-layer}}$	L_c	W_c	H_c	N_c	K_1K_2	F_c
40	8	1	150	2	1	20	1.9661	0.7097
80	4	2	150	2	1	20	0.6667	0.4061
80	3	2.5	150	2	1	20	0.6243	0.3888
80	4	2	150	2	0.5	20	0.1033	0.0886
80	4	2	150	1	1	20	0.2080	0.1641

Case1-1 or case1-2

$L_{h\text{-layer}}$	$W_{h\text{-layer}}$	$H_{h\text{-layer}}$	L_{c1}	L_{c2}	W_c	H_{c1}	H_{c2}	N_c	K_1K_2	F_c
80	4	2	20	130	2	0.5	1	20	0.3860	0.2750
80	4	2	50	100	2	0.5	1	20	0.2366	0.1852
80	4	2	75	75	2	0.5	1	20	0.1789	0.1455

Case2-0

$L_{h\text{-stack}}$	$W_{h\text{-stack}}$	$H_{h\text{-stack}}$	L_c	W_c	H_c	N_{layer}	K_1K_2	F_{layer}
100	2	18	150	2	1	20	0.1353	0.1119
100	2	18	150	2	0.5	20	0.0210	0.0187
100	2	78	150	2	1	20	0.0297	0.0264

Case2-1 or case2-2

$L_{h\text{-stack}}$	$W_{h\text{-stack}}$	$H_{h\text{-stack}}$	L_{c1}	L_{c2}	W_c	H_{c1}	H_{c2}	N_{layer}	K_1K_2	F_{layer}
100	2	18	20	130	2	0.5	1	20	0.0783	0.0671
100	2	18	50	100	2	0.5	1	20	0.0480	0.0420
100	2	18	75	75	2	0.5	1	20	0.0363	0.0321

Case3-0

$L_{h\text{-stack}}$	$W_{h\text{-stack}}$	$H_{h\text{-stack}}$	L_c	W_c	H_c	N_{layer}	K_1K_2	F_{layer}
100	8	8	150	2	1	20	0.0104	0.0094
100	4	4	150	2	1	20	0.1669	0.1351
100	4	4	150	2	0.5	20	0.0259	0.0230

Case3-1 or case3-2

$L_{h\text{-stack}}$	$W_{h\text{-stack}}$	$H_{h\text{-stack}}$	L_{c1}	L_{c2}	W_c	H_{c1}	H_{c2}	N_{layer}	K_1K_2	F_{layer}
100	4	4	20	130	2	0.5	1	20	0.0967	0.0817
100	4	4	50	100	2	0.5	1	20	0.0593	0.0515
100	4	4	75	75	2	0.5	1	20	0.0448	0.0393

term while retained the inertial term. However, with the assumption of laminar flow, Maharudrayya et al. [5] have neglected the inertial term, retaining the frictional term. The resultant analytical results can present some discrepancy in comparison with the CFD simulations without such ignorance. Since this term further reduces the pressure along the header, it should increase the flow nonuniformity. On the other hand, this flow inertial movement might cause inverse flow at the header end, causing certain increase in mass flow rate in the last several channels or layers, even breaking the monotonic distribution. Another assumption is the ignorance of local pressure losses, and even the layer-header losses within the stack formulations. Such losses might be favorable for the corresponding flow uniformity among the channels or layers by reducing K_1. These competitive factors contribute to the difference situations when comparing the CFD (without the above-mentioned assumptions) and the analytical results, according to the exact configurations and even operating parameters.

Maharudrayya et al. [5] have provided certain CFD simulations to verify the validation of their analytical formulations. Although their results exhibited good agreements, the differences can still be observed to some degree (Figs. 6 and 7 in Ref. [5]). In the first several channels, the CFD derived flow rates are somewhat higher that the analytical ones mainly due to the enhanced pressure loss by the inertial term, while in the last several channels, the CFD flow rates also give higher values and somewhat change the monotonic decreasing of the flow distribution along the feed header. Based on certain assumptions, the analytical formulation shows that in the U-type configuration, the flow distribution is independent of the Reynolds number. However, slight difference appear in the distribution plots with different Reynolds number, and higher Reynolds number gives more obvious effect from the inertial term (Fig. 7(b) in Ref. [5]).

Figs. 11 and 12 illustrate the comparison between the analytical and CFD (FLUENT^{TM} 6.0) results in the present case1-0, case1-1 and case1-2, with common header length

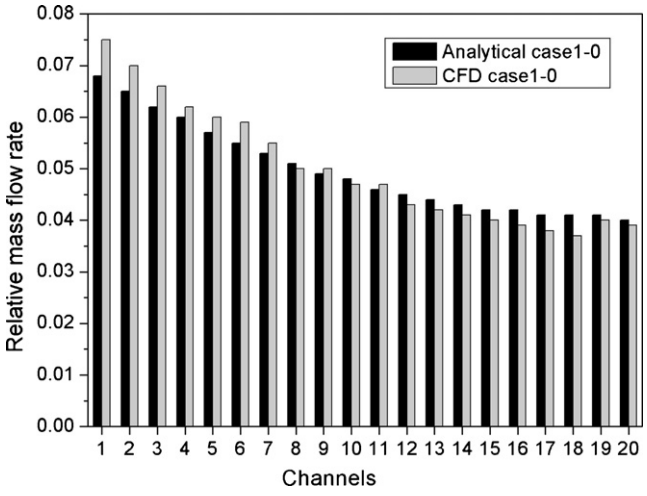

Fig. 11. Comparison of flow distribution obtained from analytical and CFD solutions in case1-0.

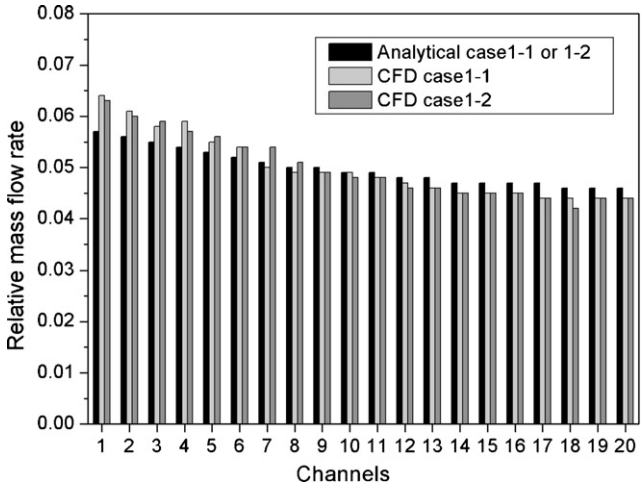

Fig. 12. Comparison of flow distribution obtained from analytical and CFD solutions in case1-1 and case1-2.

($L_{\text{h-layer}} = 80$ mm) and channel number ($N_c = 20$). Other values are $W_{\text{h-layer}} = 4$ mm, $H_{\text{h-layer}} = 2$ mm, $W_c = W_{\text{r-layer}} = 2$ mm. Additionally, $L_c = 150$ mm and $H_c = 1$ mm in case1-0, while in case1-1 and case1-2, $L_{c1} = 50$ mm (partitioned into two 25 mm in case1-1), $H_{c1} = 0.5$ mm, $L_{c2} = 100$ mm, $H_{c1} = 1$ mm. The Reynolds number was fixed at 137 for all the cases. In the present three-dimensional CFD simulations, a laminar flow was assumed with constant ρ and μ, and mass conservation (no gas consumption). The conservation equations for mass and momentum (the Navier–Stokes equations) were solved with a segregated solver, and the local losses and the inertial term were not ignored. The analytical mass flow rates were taken from the channel centers, while those in the CFD simulations were obtained via integrating over the channel cross-sections. The overall trends in the two results are in agreement, indicating the certain validation of the analytical formulations. The F_c values in case1-0 are 0.4061 and 0.5045 for the analytical and CFD results, respectively, and the last channel (no. 20) in CFD does not offer the minimum mass flow rate. This discrepancy is consistent with the reports in Ref. [5] with different layer sizes. Fig. 12 gives the results for case1-1 and case1-2. The analytical F_c is 0.1852, while CFD simulations give $F_c = 0.3160$ and 0.3323 for case1-1 and case1-2, respectively. Although the deviation is obvious, the size change in channels is found to be effective in improving the flow uniformity. And the case1-1 results from CFD show better uniformity than case1-2, indicating the pressure loss difference in the two configurations (the total pressure drops from the CFD simulations are 20.670 and 20.516 Pa for case1-1 and case1-2, respectively, and for comparison, the CFD value in case1-0 is 12.024 Pa), which has been ignored in the analytical formulations. With the reduction in header length and channel number, the deviation due to the inertial term can be expected to be more apparent. And for stack cases, the reduction in header length and layer number might lead to more severe discrepancy between the results with and without considering the inertial term, due to the large cross-sections of the stack header.

4. Conclusion

The present work extends the analytical formulations for uniform channels in a U-type layer to more complex channel structures and U-type stacks based on certain assumptions. The analytical results indicate simply that the flow distribution can be improved by reducing the pressure loss in the header (via shortening the header, expanding the hydraulic diameter of the header, reducing the channel or layer number, etc.), or increasing the pressure loss in the channels or layers (via lengthening the channels, reducing the hydraulic diameter of the channels and so on). According to the formulations, the flow-distribution uniformity among the layers in a U-type stack is easier to obtain compared with that among the channels in a U-type layer due to the larger size of stack headers usually adopted. Modifying the channel shape with narrow parts can effectively improve the flow uniformity, according to both the analytical formulations and CFD simulations. The discrepancy between the analytical and CFD results might be ascribed to whether the inertial term and local pressure losses have been ignored or not.

Acknowledgement

This work has been financially supported by the National Natural Science Foundation of China (Grant No. 50730002).

References

[1] Z. Ma, S.M. Jeter, S.I. Abdel-Khalik, J. Power Sources 108 (2002) 106–112.
[2] K.P. Recknagle, R.E. Williford, L.A. Chick, D.R. Rector, M.A. Khaleel, J. Power Sources 113 (2003) 109–114.
[3] S.W. Cha, R. O'Hayre, Y. Saito, F.B. Prinz, J. Power Sources 134 (2004) 57–71.
[4] D. Larrain, J. Van herle, F. Maréchal, D. Favrat, J. Power Sources 131 (2004) 304–312.
[5] S. Maharudrayya, S. Jayanti, A.P. Deshpande, J. Power Sources 144 (2005) 94–106.
[6] R.J. Kee, P. Korada, K. Walters, M. Pavol, J. Power Sources 109 (2002) 148–159.
[7] Y. Sung, J. Power Sources 157 (2006) 395–400.
[8] M.K. Bassiouny, H. Martin, Chem. Eng. Sci. 39 (1984) 693–700.
[9] M.K. Bassiouny, H. Martin, Chem. Eng. Sci. 39 (1984) 701–704.